# Equivalent Modal Damping of Short-Span Bridges Subjected to Strong Motion

Sungchil Lee, Ph.D.[1]; Maria Q. Feng, M.ASCE[2]; Seung-Jun Kwon, Ph.D.[3]; and Seok-Hee Hong[4]

**Abstract:** In this paper four different methods are investigated for estimating the equivalent modal damping ratios of a short-span bridge under strong ground motion by considering the energy dissipation at the boundary. The Painter Street Overcrossing (PSO) is investigated because of seismic data availability. Computed responses using the response-spectrum method with the equivalent damping ratios estimates are compared with the recorded responses. The results show that the four methods provide reasonable estimation of equivalent modal damping ratios and that neglecting off-diagonal elements in the damping matrix is the most efficient and practical method. The equivalent damping ratio of the PSO was nearly 25% under an earthquake with peak ground acceleration of 0.55*g*, which is much higher than the conventional assumption of 5%. **DOI: 10.1061/(ASCE)BE.1943-5592.0000149.** 

**CE Database subject headings:** Bridges, spans; Response spectra; Modal analysis; Vibration; California.

**Author keywords:** Bridges; Response spectra; Modal analysis.



## Introduction

Short bridges with one or two spans are mainly used to pass over a pathway. They usually have a superstructure connected directly to a wingwall, an abutment at one or both ends of the bridge, and an embankment relatively longer than the bridge length. Most often the seismic demand of short-span bridges in the design or seismic retrofit planning phase is computed based on the design (or response) spectrum method rather than on nonlinear time-history analysis. Traditionally the damping ratio of reinforced concrete bridges is assumed to be 5% for all the modes of vibration. While this assumption may be reasonable for ordinary concrete bridges, it may not be applicable to short bridges with substantial influence from the energy dissipation of the soil in abutments and supports (California Dept. of Transportation 2006). In fact, studies have shown that the modal damping ratio of a short-span bridge is higher than 5% during a strong ground motion because of the energy dissipation at the boundaries (Wilson and Tan 1990; McCallen and Romstad 1994; Goel and Chopra 1997; Goel 1997; Zhang and Makris 2001; Arici and Mosalam 2003). The damping at the bridge boundary increases the entire bridge system damping, particularly for short-span bridges, though the damping of the bridge concrete structure is assumed to be 5%. Therefore, without considering the energy dissipation at the bridge boundary, the conventional damping ratio (i.e., 5% for a concrete bridge) used in the design (or response) spectrum method for seismic design and analysis would be too conservative.

[1]Assistant Researcher, Dept. of Civil and Environmental Engineering, Univ. of California, Irvine, CA 92617. E-mail: sungcl@uci.edu

[2]Professor, Dept. of Civil and Environmental Engineering, Univ. of California, Irvine, CA 92617. E-mail: mfeng@uci.edu

[3]Assistant Researcher, Dept. of Civil and Environmental Engineering, Univ. of California, Irvine, CA 92617. E-mail: juni98@yonsei.ac.kr

[4]Vice President, Naekyung Eng. Co., Anyang-Si, Kyungki-Do, Korea 431-060. E-mail: nk2900@empal.com

Note. This manuscript was submitted on April 17, 2009; approved on June 9, 2010; published online on June 15, 2010. Discussion period open until August 1, 2011; separate discussions must be submitted for individual papers. This paper is part of the ***Journal of Bridge Engineering***, Vol. 16, No. 2, March 1, 2011. ©ASCE, ISSN 1084-0702/2011/2-316–323/$25.00.

With the additional damping from the bridge boundary, the damping matrix of an entire bridge system generally does not satisfy the Caughey-O'Kelly condition (Caughey and O'Kelly 1965), and the entire bridge system becomes nonproportionally damped and has complex eigenvalues and eigenvectors. Therefore, the modal damping ratio cannot be obtained from conventional modal analysis. Researchers have developed modal combination rules for nonproportionally damped systems to compute the seismic demand (Gupta and Jaw 1986; Villaverde 1988; Yang et al. 1990; Sinha and Igusa 1995; Falsone and Muscolino 2004; Palmeri 2006); however, those methods are complicated and difficult to integrate into the current spectrum-based design practice.

Although several studies have shown that high energy dissipation occurs at the boundaries of short-span bridges under strong ground motion (Werner et al. 1987; Price and Eberhard 2005; Kostoglou and Pantazopoulou 2007), little investigation has been performed to develop methods for computing the equivalent modal damping ratio (EMDR) with known damping at the bridge boundary. Although the modal damping ratio of a nonproportionally damped system could be found from complex modal analysis, it is not widely known to practical bridge designers. A simple and effective damping estimation method does not exist for bridge designers to use when designing and analyzing short-span bridges with additional damping at the bridge boundary.

The objective of this study is therefore to investigate four methods (complex mode analysis, neglecting off-diagonal elements in damping matrix, composite damping rule, and optimization) for computing the EMDR of nonproportionally damped bridge systems, such as short-span bridges, that can be incorporated into the current design spectrum-based method for seismic design and analysis. For the verification of the methods, the Painter Street Overcrossing (PSO) was chosen for analysis because it is a typical short-span reinforced concrete bridge and, more important, it has extensive seismic records and no structural damage.

The PSO has valuable seismic data under strong ground motion without structural failure. The seismic data offer a great opportunity for identification of equivalent linear parameters (stiffness and damping) of the bridge boundary, which are considered more accurate than the values estimated by other available methods based

on geometry and configuration of foundation and abutment (Zhang and Makris 2001; Gazetas 1991). Also, the applicability of the four damping-estimating methods can be verified by comparing the recorded responses with the results from the response-spectrum method.

The bridge boundary of the PSO is modeled with viscoelastic elements to conform to current design practice, and the properties of the viscoelastic elements are identified by using recorded seismic data. After applying the four methods, the computed EMDR of the bridge is used for the response-spectrum method. At the end of this paper, modal combination results using the EMDR from each method are compared with the recorded peak response to show the applicability of the methods in current spectrum-based design practice.

## Analysis Procedure

The analysis procedure shown in Fig. 1 was used to investigate the four damping-estimating methods. The boundary condition of the stick model was identified by using the recorded seismic data. The stick model with the equivalent viscoelastic element is a nonproportionally damped model (NP model). The nonproportional damping of the NP model is represented as the EMDR through each of the four methods. So, the NP model is approximated as a proportionally damped model (P model) with the EMDR. The stiffness matrix of both the NP model and P model is composed of the stiffness of concrete structure and the boundary; however, the damping matrix of the NP model is composed of the proportional damping of the concrete structure and the localized damping at the boundary, whereas the damping of the P model is the computed EMDR for the entire bridge system. The modal periods and mode shapes of the bridge are computed based on the P model for the response-spectrum method. Finally, modal combination rules are applied to compute the seismic demand using the modal information and the EMDR.

The accuracy of the viscoelastic element equivalent to the bridge boundary is verified by comparing the measured response and the computed time-history response from the NP model. The accuracy of the four damping-estimating methods is investigated by comparing the computed time-history responses from the NP model and the P model, since the EMDR is estimated based on the NP model.

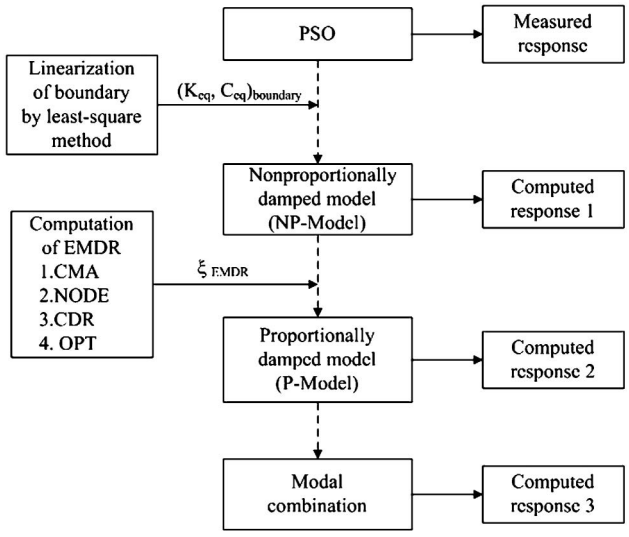


**Fig. 1.** Analysis procedure

Finally, the modal combination results are compared with the peak responses from the NP model, as well as the measured response, to investigate the applicability of the four methods to the response-spectrum method.

## Methods for Estimating Damping

For this study, the four methods were selected on the basis of their potential to estimate the equivalent modal damping of entire bridge system. They are briefly presented and discussed in this section. More details for each method are available from the references.

### *Complex Modal Analysis Method*

The equation of motion of a multi-degree-of-freedom system is

$$[m]\{\ddot{x}(t)\} + [c]\{\dot{x}(t)\} + [k]\{x(t)\} = -[m]\{i\}\{\ddot{x}_g(t)\} \quad (1)$$

where $[m]$, $[c]$, and $[k]$ are mass, damping, and stiffness matrix, respectively; $\{\ddot{x}(t)\}$, $\{\dot{x}(t)\}$, $\{x(t)\}$ are the acceleration, velocity and displacement vector at each node; $\{i\}$ is the influence vector; and $\{\ddot{x}_g(t)\}$ is the input ground motion acceleration.

In the case of nonproportionally damped systems, Eq. (1) can be decoupled using the complex-modal analysis by introducing the state space variables $\{z\} = \{^{\{\dot{x}\}}_{\{x\}}\}$ (Veletsos and Ventura 1986). Then Eq. (1) can be rewritten as

$$[A]\{\dot{z}\} + [B]\{z\} = \{Y(t)\} \quad (2)$$

in which

$$[A] = \begin{bmatrix} [0] & [m] \\ [m] & [c] \end{bmatrix}, \qquad [B] = \begin{bmatrix} -[m] & [0] \\ [0] & [k] \end{bmatrix},$$

$$[Y(t)] = \begin{Bmatrix} \{0\} \\ -[m]\{i\}\ddot{x}_g(t) \end{Bmatrix}$$

Assuming that the homogeneous solution of Eq. (2) is of the form $\{x\} = \{\psi\}e^{st}$, Eq. (2) becomes

$$s([A] + [B])\{z\} = \{0\} \quad (3)$$

The eigenvalues of Eq. (3) are complex conjugate pairs. Let $s_i$ and $\bar{s}_i$ be a conjugate pair of eigenvalues; then

$$\left.\begin{matrix} s_i \\ \bar{s}_i \end{matrix}\right\} = -\sigma \pm i\omega_D = -\omega_i\xi_i \pm i\omega_i\sqrt{1-\xi_i^2} \quad (4)$$

The natural frequency and the EMDR are obtained from Eq. (4) by Eqs. (5) and (6)

$$\omega_i = \sqrt{(\mathrm{Re}(s_i))^2 + (\mathrm{Im}(s_i))^2} \quad (5)$$

$$\xi_i = \frac{\mathrm{Re}(s_i)}{\omega_i} \quad (6)$$

### *Neglecting Off-Diagonal Elements Method*

The pre- and postmultiplication of normal mode shape to nonproportional damping matrix is

$$[\Phi]^T[c][\Phi] = \begin{bmatrix} \{\phi_1\}^T[c]\{\phi_1\} & \cdots & \{\phi_1\}^T[c]\{\phi_n\} \\ \vdots & \ddots & \vdots \\ \{\phi_n\}^T[c]\{\phi_1\} & \cdots & \{\phi_n\}^T[c]\{\phi_n\} \end{bmatrix} \quad (7)$$

in which $\{\phi_i\}$ is the $i$th normal mode shape and $[c]$ is a nonproportional damping matrix.



J. Bridge Eng. 2011.16:316-323.

In this method, the off-diagonal elements of Eq. (7) are neglected and the EMDR is computed by

$$\xi_i = \frac{\{\phi_i\}^T[c]\{\phi_i\}}{2\{\phi_i\}^T[m]\{\phi_i\}\omega_i} \tag{8}$$

where $\xi_i$ is the $i$th EMDR. Because the off-diagonal elements are eliminated in Eq. (7), the accuracy of this method depends on the modal coupling of each pair of modes. Warburton and Soni (1977) proposed a parameter to quantify the modal coupling for this method as follows:

$$e_{i,j} = \frac{\{\phi_i\}^T[c]\{\phi_j\}\omega_i}{|\omega_i^2 - \omega_j^2|} \tag{9}$$

where $e_{i,j}$ is the modal coupling parameter and $\omega_i$ and $\omega_j$ are the $i$th and $j$th natural frequency, respectively. If the parameter $e_{i,j}$, which means the modal coupling of the $i$th and $j$th modes, is small enough relative to unity for all pairs of modes, the approximation by this method yields quite accurate results.

### *Optimization Method*

The optimization in the time domain and frequency domain is used to compute the EMDR. In this method, the EMDR of the NP model is updated through iterations to produce the similar damping effect of the NP model through iterations. First, the initial EMDR is assumed and a ground motion is applied to the P model and the NP model. The computed responses from the P model and the NP model are compared. Therefore, the optimization method in time domain requires the direct numerical integration method to compute the response under ground motion. Through iterations the EMDR of the P model is updated to minimize an objective function, as shown in Eq. (10)

$$F = \min\left[\sum_i (x_i^{np} - x_i^p)^2\right] \tag{10}$$

in which $x_i^{np}$ and $x_i^p$ are the computed response from the NP model and P model at the $i$th time step, respectively.

The time-history analysis of the time domain optimization method can be avoided in the frequency domain by constituting the objective function with the frequency response function of the NP model and P model, as shown in Eq. (11). The objective function in the frequency domain is

$$F = \min\left[\sum_i [H^{np}(j\omega_i) - H^p(j\omega_i)]^2\right] \tag{11}$$

where $H^{np}(j\omega_i)$ and $H^p(j\omega_i)$ are the frequency response function of the NP model and P model at frequency, respectively.

### *Composite Damping Rule Method*

The composite damping rule was suggested for the computation of the EMDR of building structures with different damping components (Raggett 1975). The basic assumption of this method is that the total dissipated energy of a linear system with different viscous elastic damping components is the sum of the dissipated energy from each component. In this method, the EMDR of the $i$th mode is computed as Eq. (12)

$$\xi_i = \sum_j \xi_j \frac{U_{j,i}}{U_{t,i}} \tag{12}$$

in which $\xi_j$ is the damping ratio of the $j$th component; $U_{j,i}$ is the $i$th modal potential energy of the $j$th component; and $U_{t,i}$ is the $i$th modal potential energy of the total system. Eq. (12) shows that the EMDR equals the sum of the damping ratios of each component, weighted by the ratio of each component's potential energy to the total potential energy of the system.

## Painter Street Overcrossing

The PSO, located in Rio Dell, California, was selected for analysis in this study because this short-span bridge has experienced many recorded earthquakes. The PSO, shown in Fig. 2, consists of a continuous reinforced concrete multicell box girder deck and is supported with integral abutments at the two ends and a two-column center bent. It has two unequal spans of 36.3 m (119 ft) and 44.5 m (146 ft). Both abutments are skewed at an angle of 38.9°. The deck is connected to the abutment at the east side but is seated on the pile cap of the abutment at the west side.

The monitoring system has recorded nine earthquakes since installation of strong motion sensors in 1977. However, this paper only analyzes the strongest earthquake on record (Cape Mendocino/Petrolina earthquake in 1992). During the earthquake, the peak ground acceleration in the longitudinal and transverse directions was $0.38g$ and $0.55g$, respectively. Other seismic records have much less intense ground motion. No structural damages to the columns and concrete structures were found during the post-earthquake investigation by Caltrans, which implies that the structural components remained in the elastic range. If a column or abutment of the bridge failed during the earthquake, the analysis procedure adopted in this study cannot be meaningful because, in that case, most of the damping of the entire bridge would be attributed to the hysteretic damping of the damaged structure components, which is not accounted for in seismic design. However, since the bridge and abutment did not crack or fail under the ground motion, the bridge components behaved in the elastic range with high damping from the abutment.

## Finite-Element Model of the PSO

Although the recorded acceleration at the top of the column bent was $0.86g$ in transverse direction, the bridge did not suffer any structural damage during the earthquake, which implies that the

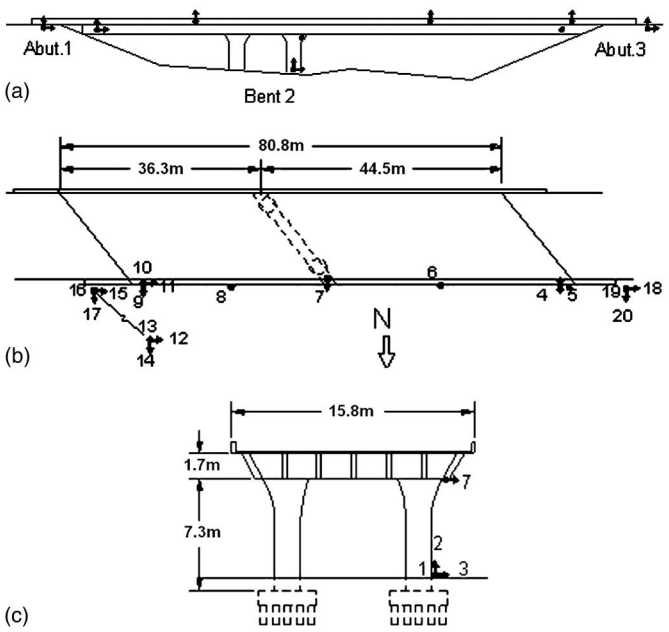


**Fig. 2.** Painter Street Overcrossing and sensor locations: (a) elevation; (b) deck level plan; and (c) section at bent



J. Bridge Eng. 2011.16:316-323.

structural components remained elastic. All elements are assumed as linear elastic for the response-spectrum method.

### Modeling of Bridge Structure

Fig. 3 shows a stick model of the PSO. The writers of this study developed a computer program to create this model because the four damping-estimating methods require a physical model of the bridge (i.e., mass, stiffness, and damping matrix cannot be extracted from other commercial structural analysis software). This program can handle the Rayleigh damping and nonclassical damping from the bridge boundary. Because the analysis uses linear-elastic elements, a nonlinear solver is not needed for this program.

The deck and bent are composed of 10 and 4 linear elastic beam elements, respectively. Each node has two degrees of freedom: translation in the $y$-direction for all the nodes and rotation along the $z$-axis for deck nodes (Nodes 1 to 11) and rotation along the $x$-axis for bent nodes (Nodes 12 to 15). The two columns comprising the center bent are combined as one member in the finite-element model. The spring and damper at the boundary are assumed only in the $y$-direction. The rotation at the bottom of the bent is assumed to be fixed. Table 1 shows the element property of the finite-element model. The cross sections of the column and deck are assumed uncracked. The Young's modulus of concrete is assumed equal to 80% of the initial design value considering the aging effect (Zhang and Makris 2001). The damping of the reinforced concrete structure is assigned as 5% Rayleigh damping.

### Modeling of Bridge Boundary

Although the bridge structure is thought to remain in the elastic range, Goel and Chopra (1997) observed that the bridge may respond in the nonlinear range during an earthquake because of nonlinearities at the abutment soil pile systems from the identified force-displacement curve at the embankment of the bridge. The abutment-embankment system can be modeled in various ways, from a single linear or nonlinear spring to a combination of series and parallel linear and nonlinear springs. The lateral stiffness at the abutment is attributed to abutment piles, shear keys, soil-structure interactions, and seat type of the deck. However, in this study, the lateral stiffness at the abutment was not based on a nonlinear model of all the components. Instead, the bridge boundary condition was represented by an equivalent viscoelastic element, since the abutment soil did not fail during the earthquake and it is more appropriate than a nonlinear element for the response-spectrum method.

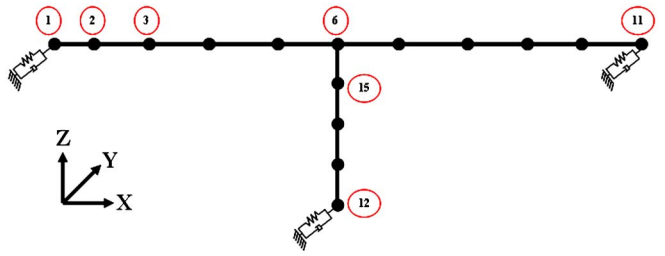


**Fig. 3.** Finite-element model of Painter Street Overcrossing

**Table 1.** Element Properties of PSO

| Properties | Deck | Column |
|---|---|---|
| Mass density | 2,400 kg/m$^3$ | 2,400 kg/m$^3$ |
| Young's modulus | 22 GPa | 22 GPa |
| Area | 8.29 m$^2$ | 1.92 m$^2$ |
| Moment of inertia | 153.90 m$^4$ | 0.29 m$^4$ |

**Table 2.** Spring Stiffness and Damping Coefficient of Boundary

| Location | Spring stiffness (MN/m) | Damping coefficient (MN·s/m) |
|---|---|---|
| East abutment | 78 | 5 |
| West abutment | 78 | 5 |
| Bent | 642 | 5 |

The properties of the equivalent viscoelastic element (i.e., spring stiffness and viscous damping coefficient) were identified based on least-square optimization using the recorded seismic response data for the bridge. The free-field ground motion in the transverse direction (Channel 14 in Fig. 2) was used as an input ground motion and the response at the top of the bent (Channel 7 in Fig. 2, and Node 6 in Fig. 3) was chosen as a reference. Because of a weak wave-scatter field, the recorded free-field earthquake record was assumed at the foundation level. This is consistent with the assumptions made by previous researchers for the same structure (Makris et al. 1994).

The objective function is constituted with the relative errors of the response time-history and power spectral density functions from the measured and computed response (Li and Mau 1991), as shown in Eq. (13). Over iterations, effective stiffness and damping coefficient values are updated to minimize the objective function

$$F = \frac{\sum_i (x_i^m - x_i^c)^2}{\sum_i (x_i^m)^2} + \frac{\sum_j \{p^m(\omega_j) - p^c(\omega_j)\}^2}{\sum_j \{p^m(\omega_j)\}^2} \tag{13}$$

where $F$ is the objective function; $x_i$ is the response at the $i$th time step; $p(\omega_j)$ is the power spectral density of the response at frequency $\omega_j$; and superscript $m$ and $c$ are the measured response and computed response, respectively.

Table 2 shows the equivalent linear spring stiffness and viscous damping coefficient values of the PSO boundaries from the least-square method. Figs. 4 and 5 show the time-history and power spectral density of the measured and computed responses at the top of the bent. From the figures, the calculated response and power spectral density show good agreement with the measured ones. Therefore, the viscoelastic model is believed to represent the abutment-embankment system well. The values in Table 2 are adopted as the boundary conditions of the PSO. The stick model of the PSO in Fig. 3 is a nonproportionally damped system because of the damping at the boundary, though the damping of the concrete structure is proportional.

The updating procedure described here can be used only for bridges with recorded seismic data. In the design of new bridges or analysis of existing bridges without recorded seismic data, the equivalent linear damping and stiffness of the bridge boundary can be computed by available methods such as Zhang and Makris (2001) or Gazetas (1991).

## Analysis Results

Based on the nonproportionally damped model of the PSO, each of the four methods is applied to estimate the EMDR. The concrete structure part of the PSO is assumed as 5% Rayleigh damping. The acceleration and displacement responses computed from the NP model and P model are compared with the measured response. The responses of the P model are computed by using the modal



J. Bridge Eng. 2011.16:316-323.

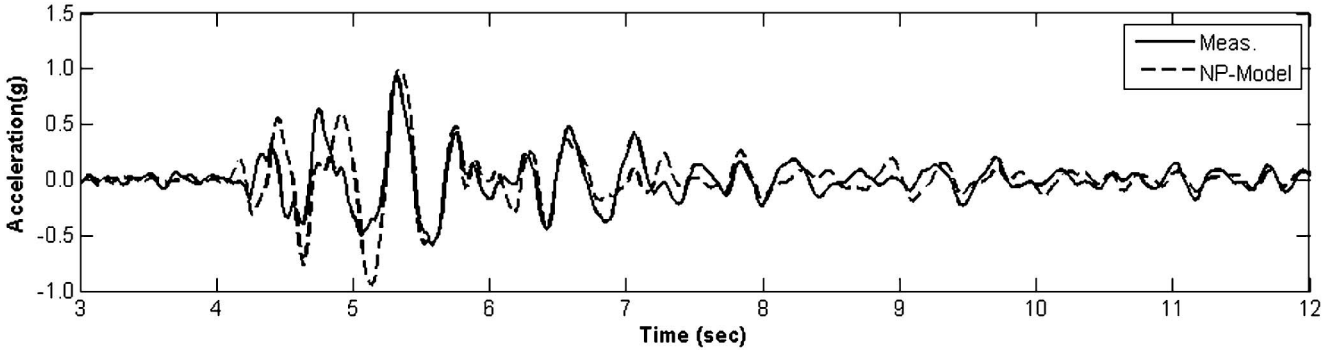


**Fig. 4.** Acceleration time-history response

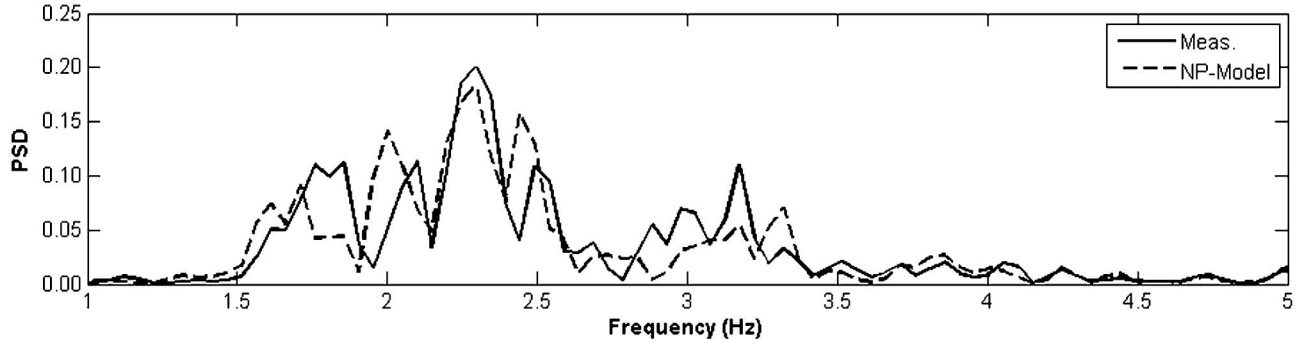


**Fig. 5.** Power spectral density of acceleration at top of bent



superposition method and with the EMDR identified from each of the four methods. The summary of the identified EMDR and peak values of the acceleration and displacement are summarized in Tables 3 and 4. In Table 4, the values in parentheses are peak displacement responses in centimeters.

### *Complex Modal Analysis Method*

The NP model was analyzed with a complex modal analysis to determine the EMDR and modal frequencies of the PSO. Table 5 shows the undamped modal frequency of the NP model and the P model of the PSO. The modal frequency of the NP model is computed from Eq. (5). Table 5 shows that modal frequencies of both models in the transverse direction are very close to each other up to the fourth mode. From Eq. (6), the first and the second modal-damping ratios are found as 25 and 55%, respectively (Table 3).

The acceleration and displacement time history at the top of the bent is shown in Fig. 6. The response plots from all other methods are very similar to the plots in Fig. 6 because of small differences in EMDR. The errors of peak response values between the two models are less than 10% (Table 4). The response of the P model shows a good agreement between the NP model response and the measured data.

**Table 3.** Summary of Identified EMDR

| | | | OPT | | |
|---|---|---|---|---|---|
| Mode | CMA | NODE | Time domain | Frequency domain | CDR |
| 1 | 0.248 | 0.245 | 0.252 | 0.242 | 0.195 |
| 2 | 0.551 | 0.544 | 0.205 | 0.197 | 0.245 |
| 3 | 0.307 | 0.299 | 0.252 | 0.242 | 0.087 |
| 4 | 0.195 | 0.194 | 0.543 | 0.522 | 0.055 |
| 5 | 0.316 | 0.367 | 0.678 | 0.651 | 0.155 |

### *Neglecting Off-Diagonal Element Method*

To apply this method, the damping matrix of the bridge should first be established. After pre- and postmultiplication of the normal mode shape to the damping matrix the off-diagonal elements are neglected and the EMDR of each mode is calculated by using Eq. (8). The computed responses from the P model with the EMDR from this method are almost the same as those from the complex modal analysis method. From Table 3, the EMDR of each mode from this method is very close to those from the complex modal analysis method, and the relative error of acceleration and displacement is less than 8%.

### *Optimization Method*

In the optimization method, the damping of the P model is assumed as Rayleigh damping, and the first and third modal damping ratios are set to be equal. In the time domain, optimization of the acceleration response at the top of the bent of the nonproportionally damped and proportionally damped model is used for the objective function, whereas the frequency response function at the same location is used in the frequency domain.

From Table 3, the EMDR from both the time domain and the frequency domain are very close to each other. The large discrepancy in the EMDR after the fourth mode through the optimization method in Table 3 is attributed to the assumption of Rayleigh damping for the P model. Nevertheless, the overall responses from the optimization method are not so different from the complex modal analysis method results because of the high modal contribution of the first mode. The relative error between the P model and the NP model is less than 10%.

**Table 4.** Measured and Computed Peak Acceleration ($g$) and Displacement (cm) Responses

| Method | Measured | Computed | | Relative error[c] | |
|---|---|---|---|---|---|
| | | NP model | P model | (NP-P)/P | (Measured-P)/P |
| CMA | 0.942 (5.553) | 1.031 (6.098) | 0.941 (5.662) | 0.096 (0.077) | 0.001 (−0.019) |
| NODE | | | 0.947 (5.706) | 0.089 (0.069) | −0.005 (−0.027) |
| OPT[a] | | | 0.937 (5.622) | 0.100 (0.085) | 0.005 (−0.012) |
| OPT[b] | | | 0.954 (5.758) | 0.081 (0.059) | −0.013 (−0.036) |
| CDR | | | 1.068 (6.478) | −0.035 (−0.058) | −0.112 (−0.142) |

[a]Optimization method in time domain.
[b]Optimization method in frequency domain.
[c]NP: results from NP model; P: results from P model.

**Table 5.** Modal Frequency of PSO

| Mode | Undamped modal frequency (Hz) | |
|---|---|---|
| | NP model | P model |
| 1 | 1.742 | 1.695 |
| 2 | 2.681 | 2.653 |
| 3 | 7.194 | 7.341 |
| 4 | 18.624 | 18.833 |
| 5 | 27.166 | 23.823 |

### *Composite Damping Rule Method*

All the previous methods require damping coefficient values at the boundaries, whereas the composite damping rule (CDR) method needs the damping ratios of each different damping component. According to the basic principle of this method, the PSO is divided into two different damping components: (1) the reinforced concrete structure component of the deck and bent and (2) the boundary component. The damping ratio of the reinforced concrete components is assumed as 5% and that of the boundary as 25% (Kostoglou and Pantazopoulou 2007).

After computing the modal potential energy and the energy ratio of the concrete structure and boundary components, the EMDR is computed by using Eq. (12), and is shown in Table 3. Although the EMDR from the composite damping rule method is lower than that of other methods, the time-history responses are very close to the measured and the NP model response, because the EMDR from the CDR method and other methods is high enough and the small variance in the EMDR makes little difference in the responses.

## Modal Combination Results

To investigate the applicability of the four methods to the current practical spectrum-based method, the modal combination rules such as absolute sum (ABSSUM), square root of sum of squares (SRSS) and complete quadratic combination (CQC) are used with the EMDR from each method and the modal information of the P model. Table 6 shows the modal combination results of acceleration and displacement at the top of the bent. The values in parentheses are displacements. The first five modes are used for the modal combination. The last row of the table is the computed response, assuming the conventional 5% modal damping ratio for each mode. The results from the conventional 5% modal damping ratio are nearly

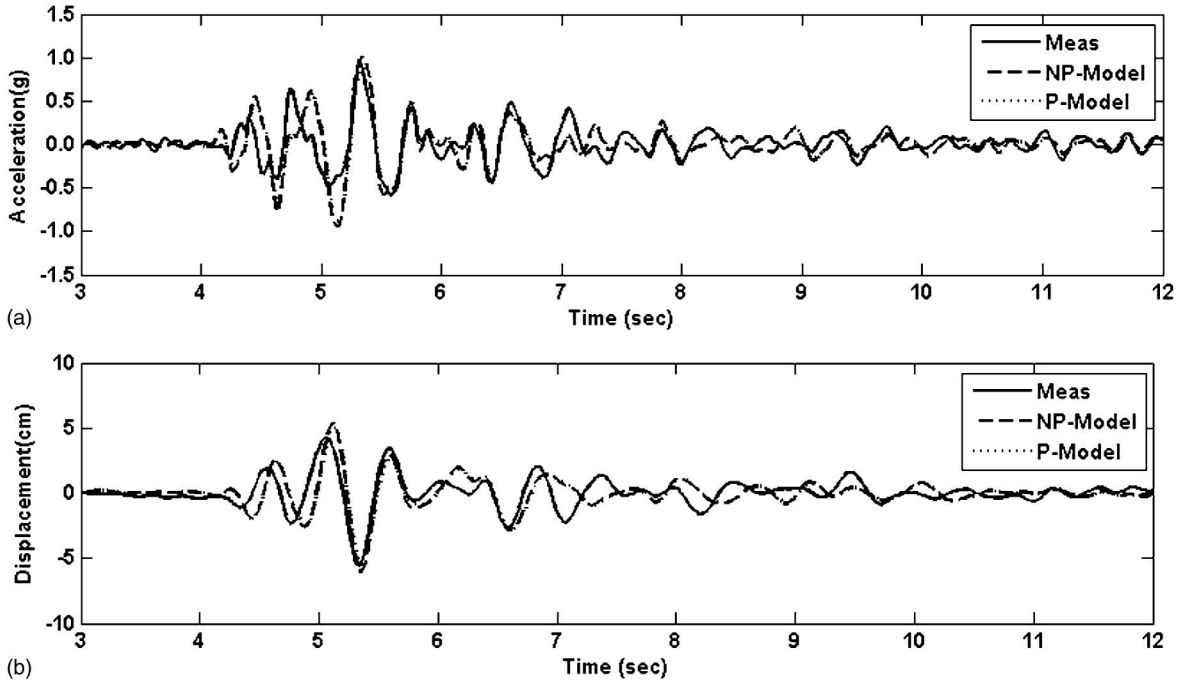


**Fig. 6.** Response at top of bent from complex modal analysis method: (a) acceleration and (b) displacement



J. Bridge Eng. 2011.16:316-323.

**Table 6.** Modal Combination Results of Acceleration ($g$) and Displacement (cm)

| Method | ABSSUM | SRSS | CQC | NP model | Measured |
|---|---|---|---|---|---|
| CMA | 0.957 (5.201) | 0.925 (5.089) | 0.942 (5.157) | 1.087 (5.725) | 0.942 (5.553) |
| NODE | 0.944 (5.126) | 0.918 (5.053) | 0.928 (5.095) | | |
| OPT[a] | 0.980 (5.298) | 0.939 (5.053) | 0.957 (5.095) | | |
| OPT[b] | 0.967 (5.771) | 0.951 (5.745) | 0.952 (5.745) | | |
| CDR | 1.196 (6.615) | 1.148 (6.497 | 1.164 (6.559) | | |
| EMDR = 5% | 1.960 (10.962) | 1.876 (10.750) | 1.911 (10.886) | | |

[a]Optimization method in time domain.
[b]Optimization method in frequency domain.



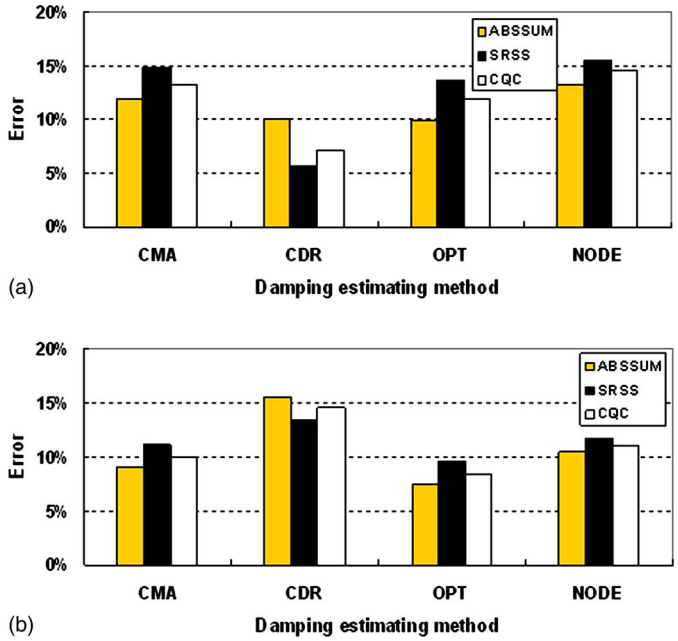


**Fig. 7.** Relative error of modal combination results with measured NP model response: (a) acceleration and (b) displacement

two times that of the measured responses. From this result, it can be concluded that the assumed 5% modal damping ratio is too conservative for the seismic design of short-span bridges with substantial energy dissipation from the boundary.

Fig. 7 shows the relative errors of the modal combination results with the peak response values from the NP model. The relative errors are less than 15% for all methods. Considering that the modal combination rules are based on random vibration theory, the relative errors are quite tolerable. The results from the neglecting off-diagonal element method are very close to those from the complex modal analysis method, both in acceleration and displacement.

The modal damping ratio as high as 25% for the PSO under the strong earthquake is verified by comparing the results from the response-spectrum method and the recorded seismic responses. The high modal damping ratio was also identified by Arici and Mosalm (2003) for the same bridge under the same earthquake, although the identified damping ratio was dependent on a parameter of the system identification method that they applied.

## Conclusions

To develop a procedure for reasonably estimating equivalent damping ratios that takes into consideration the energy dissipation in the boundaries, this study investigated the four methods on an example short-span concrete bridge, the PSO, which has recorded seismic data. In this study, the boundary condition, represented by viscoelastic elements, of a bridge system was identified on the basis of seismic data.

This study confirms that the damping ratio, 5%, used in the current response-spectrum based seismic design and analysis underestimate the system damping of a short-span bridge. The energy dissipation at the bridge boundaries makes a significant contribution to the damping of the entire bridge system under a strong ground motion. The equivalent modal damping ratio of the PSO under the strong earthquake was found to be as high as 25%, which is consistent with the results obtained by Arici and Mosalam (2003). They studied the same bridge under the same excitation, and the equivalent modal damping ratio was found to be as high as 20 to 35%, depending on the different parameters of their system-identification method.

The responses computed from time-history analysis and modal analysis of the equivalent proportionally damped system using the estimated EMDR are compared with those from the nonproportionally damped model and the measured responses. On the basis of the results obtained from this study, in general, all of the four methods provide a reasonable estimation of the EMDR. The pros and cons of each method are summarized below:

1. The complex modal analysis method estimates the EMDR with the highest accuracy. However, to apply this method in the design practice, complex-valued eigen analysis must be conducted.
2. The accuracy of the neglecting off-diagonal element method depends on the significance of modal coupling. Normal mode shapes of a bridge system should be computed to establish a generalized damping matrix before eliminating the off-diagonal elements of the matrix. However, this method is easy to apply and does not require the complicated computations that the complex modal analysis method does.
3. To apply the optimization method, the optimization routine should be executed with the bridge model. In the time domain, direct numerical integration is inevitable, whereas the frequency domain requires only the frequency response function of a nonproportionally damped and proportionally damped model. In addition, the frequency response functions of both models should be close to each other to guarantee accurate results.
4. In the composite-damping rule method, the energy ratio and damping ratio of each component must be given. Also, mode shapes are needed to compute the modal strain energy of each component and the total system. So the damping ratio, instead of the damping coefficient, of the bridge boundaries is needed to estimate the EMDR, and the damping ratio is difficult to obtain in practice.

In summary, the four damping-estimating methods produced consistent EMDR-estimation results, but the neglecting off-diagonal element method is considered the most efficient and practical method because it is simple, easy to implement, and produces a highly accurate estimation of the EMDR.

Although the observations made in this study are based on analysis of one short-span bridge under a specific seismic event, because of the limited recorded seismic data under strong motion without structural damages, the method adopted in this study can be used to identify the equivalent damping ratio of other bridges under other intensities of ground motion.

## Acknowledgments

The study presented in this paper was supported by the California Department of Transportation (Caltrans) under Grant No. 59A0495, the NaeKyung Engineering Company, and the Infra-Structures Assessment Research Center (ISARC) funded by the Ministry of Land, Transport, and Maritime Affairs, Korea. The writers would like to thank Dr. Joseph Penzien, Professor Emeritus at University of California, Berkeley, and Mr. Mike Keever and Mr. Lihong Sheng of Caltrans for their guidance and support.

## References

Arici, Y., and Mosalam, M. (2003). "System identification of instrumented bridge systems." *Earthquake Eng. Struct. Dyn.*, 32, 999–1020.

California Dept. of Transportation. (2006). *Seismic design criteria*, Version 1.4, Division of Engineering Services, Sacramento, CA.

Caughey, T. K., and O'Kelly, M. E. J. (1965). "Classical normal modes in damped linear dynamic systems." *J. Appl. Mech.*, 32, 583–588.

Falsone, G., and Muscolino, G. (2004). "New real-value modal combination rules for non-classically damped structures." *Earthquake Eng. Struct. Dyn.*, 33, 1187–1209.

Gazetas, G. (1991). "Foundation vibrations." *Foundation Engineering Handbook*, 2nd Ed., H.-Y. Fang, ed., Van Nostrand Reinhold, New York, 553–593.

Goel, R. K. (1997). "Earthquake characteristics of bridges with integral abutments." *J. Struct. Eng.*, 123(11), 1435–1443.

Goel, R. K., and Chopra, A. K. (1997). "Evaluation of bridge abutment capacity and stiffness during earthquakes." *Earthquake Spectra*, 13(1), 1–23.

Gupta, A. K., and Jaw, J. W. (1986). "Response spectrum method for non-classically damped system." *Nucl. Eng. Des.*, 91, 161–169.

Kotsoglou, A., and Pantazopoulou, S. (2007). "Bridge-embankment interaction under transverse ground excitation." *Earthquake Eng. Struct. Dyn.*, 36(12), 1719–1740.

Li, Y., and Mau, S. T. (1991). "A case study of MIMO system identification applied to building seismic records." *Earthquake Eng. Struct. Dyn.*, 20, 1045–1064.

Makris, N., Badoni, D., Delis, E., and Gazetas, G. (1994). "Prediction of observed bridge response with soil-pile-structure interaction." *J. Struct. Eng.*, 120(10), 2992–3011.

McCallen, D. B., and Romstad, K. M. (1994). "Dynamic analyses of a skewed short-span, box-girder overpass." *Earthquake Spectra*, 10(4), 729–755.

Palmeri, A. (2006). "Correlation coefficients for structures with viscoelastic dampers." *Eng. Struct.*, 28, 1197–1208.

Price, T. E., and Eberhard, M. O. (2005). "Factors contributing to bridge-embankment interaction." *J. Struct. Eng.*, 131(9), 1345–1354.

Raggett, J. D. (1975). "Estimating damping of real structures." *J. Struct. Div.*, 101(9), 1823–1835.

Sinha, R., and Igusa, T. (1995). "CQC and SRSS methods for non-classically damped structures." *Earthquake Eng. Struct. Dyn.*, 24, 615–619.

Veletsos, A. S., and Ventura, C. E. (1986). "Modal analysis of non-classically damped linear systems." *Earthquake Eng. Struct. Dyn.*, 14, 217–243.

Villaverde, R. (1988). "Rosenblueth's modal combination rule for systems with non-classically damping." *Earthquake Eng. Struct. Dyn.*, 16, 315–328.

Warburton, G. B., and Soni, S. R. (1977). "Errors in response calculations for non-classically damped structures." *Earthquake Eng. Struct. Dyn.*, 5, 365–376.

Werner, S. D., Beck, J. L., and Levine, M. B. (1987). "Seismic response evaluation of Meloland Road Overpass using 1979 Imperial Valley earthquake records." *Earthquake Eng. Struct. Dyn.*, 15, 249–274.

Wilson, J. C., and Tan, B. S. (1990). "Bridge abutments: Formulation of simple model for earthquake response analysis." *J. Eng. Mech.*, 116(8), 1828–1837.

Yang, J. N., Sarkani, S., and Long, F. X. (1990). "A response spectrum approach for seismic analysis of nonclassically damped structures." *Eng. Struct.*, 12, 173–184.

Zhang, J., and Makris, N. (2001). "Seismic response analysis of highway overcrossings including soil-structure interaction." *Rep. No. UCB/PEER 2001/02*, Pacific Earthquake Engineering Research Center, Berkeley, CA.